THE ASTRONOMICAL JOURNAL, 116:723–737, 1998 August

AGES AND METALLICITIES OF STAR CLUSTERS AND SURROUNDING FIELDS IN THE OUTER DISK OF THE LARGE MAGELLANIC CLOUD

EDUARDO BICA
Departamento de Astronomia, Instituto de Física, Universidade Federale do Rio Grande do Sul, C.P. 15051, 91501-970 Porto Alegre, RS, Brazil
DOUG GEISLER
Kitt Peak National Observatory, National Optical Astronomy Observatories, P.O. Box 26732, Tucson, AZ 85726
HORACIO DOTTORI
Departamento de Astronomia, Instituto de Física, Universidade Federale do Rio Grande do Sul, C.P. 15051, 91501-970 Porto Alegre, RS, Brazil
JUAN J. CLARIÁ[1] AND ANDRÉS E. PIATTI[1]
Observatorio Astronómico de Córdoba, Laprida 854, 5000 Córdoba, Argentina
AND
JOÃO F. C. SANTOS, JR.
Departamento de Física, Instituto de Ciências Exatas, Universidade Federale de Minas Gerais, C.P. 702, 30123-970 Belo Horizonte, MG, Brazil
Received 1998 January 16; revised 1998 March 11

ABSTRACT

We present Washington system CT_1 color-magnitude diagrams of 13 star clusters and their surrounding fields that lie in the outer parts of the LMC disk ($r > 4°$), as well as a comparison inner cluster. The total area covered is large ($\frac{2}{3}$ deg^2), allowing us to study the clusters and their fields individually and in the context of the entire Galaxy. Ages are determined by means of the magnitude difference δT_1 between the giant branch clump and the turnoff, while metallicities are derived from the location of the giant and subgiant branches as compared with fiducial star clusters. This yields a unique data set in which ages and metallicities for both a significant sample of clusters and their fields are determined homogeneously. We find that in most cases the stellar population of each star cluster is quite similar to that of the field where it is embedded, sharing its mean age and metallicity. The old population ($t \geq 10$ Gyr) is detected in most fields as a small concentration of stars on the horizontal branch blueward and faintward of the prominent clump. Three particular fields present remarkable properties: (1) The thus-far unique cluster ESO 121-SC03 at $\approx$9 Gyr has a surrounding field that shares the same properties (which, in turn, is also unique, in that such a dominant old-field component is not present elsewhere—at least not significantly in the fields as yet studied). (2) The field surrounding the far eastern intermediate-age cluster OHSC 37 is noteworthy in that we do not detect any evidence of LMC stars: it is essentially a Galactic foreground field. We can thus detect the LMC field out to greater than 11° (the deprojected distance of ESO 121-SC03), or $\sim$11 kpc, but not to 13° ($\sim$13 kpc), despite the presence of clusters at this distance. (3) In the northern part of the LMC disk, the fields of SL 388 and SL 509 present color-magnitude diagrams with a secondary clump $\approx$0.45 mag fainter than the dominant intermediate-age clump, suggesting a stellar population component located behind the LMC disk at a distance comparable to that of the SMC. Possibly we are witnessing a depth effect in the LMC, and the size of the corresponding structure is comparable to the size of a dwarf galaxy. The unusual spatial location of the cluster OHSC 37 and the anomalous properties of the SL 388 and SL 509 fields might be explained as debris from previous LMC interactions with the Galaxy and/or the SMC. The mean metallicity derived for the intermediate-age outer disk clusters is $\langle$[Fe/H]$\rangle = -0.66$, and for their surrounding fields $\langle$[Fe/H]$\rangle = -0.56$. These values are significantly lower than those found by Olszewski et al. for a sample of clusters of similar age but are in good agreement with several recent studies. A few clusters stand out in the age-metallicity relation, in that they are intermediate-age clusters at relatively low metallicity ([Fe/H] ≈ -1).

Key words: galaxies: star clusters — Magellanic Clouds

1. INTRODUCTION

Unveiling the star formation history and chemical enrichment of galaxies is critical to the development of an understanding of how they form and evolve. In this respect, Local Group galaxies play a fundamental role (Hodge 1989). The proximity of the Large Magellanic Cloud allows the probing of its stellar population properties with different techniques, namely, photometry and spectroscopy of individual stars in clusters and the field, and integrated methods in the case of star clusters. Such studies of nearby galaxies are important to better understand very distant galaxies, whose stellar populations can only be probed by means of integrated properties.

Concerning field color-magnitude diagram (CMD) studies, ground-based observations have allowed the accurate study of the brighter evolutionary sequences, sampling relatively large fields throughout the LMC bar and disk

[1] Visiting Astronomer, Cerro Tololo Inter-American Observatory, National Optical Astronomy Observatories, operated by the Association of Universities for Research in Astronomy, Inc., under cooperative agreement with the National Science Foundation.

(e.g., Butcher 1977; Hardy et al. 1984; Bertelli et al. 1992; Westerlund, Linde, & Lyngå 1995; Vallenari et al. 1996). A prominent intermediate-age (1–3 Gyr) stellar population is universally present in these fields, together with varying amounts of young blue main-sequence (MS) stars. *Hubble Space Telescope* (*HST*) observations are limited to a small viewing area but, in turn, allow deeper photometry, to well below the old MS turnoff. Several such fields have been studied with the V and I bands. One, at $\approx 4°$ north of the bar (Gallagher et al. 1996), and another near the southeast end of the bar (Elson, Gilmore, & Santiago 1997) show evidence of the major star-forming event having occurred ≈ 2 Gyr ago, in agreement with the ground-based studies. More recent *HST* studies (Holtzman et al. 1997; Geha et al. 1998) have investigated three LMC fields at 3°–4° from the bar center, one located in the northeast and two in the northwest. Surprisingly, they are finding many more faint MS stars than expected and suggest that there has been more star formation in the past than previously believed. Their models, assuming a standard IMF slope, suggest that fully one-half of the stars in these fields were formed more than 4 Gyr ago. Although the latter studies refer to their fields as "outer," we point out that in the present work we deal with genuine outer disk fields, well beyond any of these *HST* studies.

Integrated photometry of large star cluster samples of all ages have shown differences in the spatial distribution of age groups both in the bar region (Bica, Clariá, & Dottori 1992) and the entire LMC (Bica et al. 1996). Differences in the spatial distribution among young groups have provided insight on the formation process and subsequent dynamical evolution of star cluster generations (Dottori et al. 1996). This integrated photometry cluster sample has been compared with integrated star cluster color models and has provided constraints on the cluster formation history (Girardi & Bica 1993; Girardi et al. 1995).

CMDs of LMC star clusters have also revealed a large intermediate-age population, which is separated by a pronounced age gap from the old stellar population as represented by a few genuine globular clusters (see Da Costa 1991; Suntzeff et al. 1992; Olszewski, Suntzeff, & Mateo 1996 for reviews). Recently, CMDs in the Washington system of a sample of candidate old clusters selected from the Bica et al. (1996) and Olszewski et al. (1991) studies revealed them to instead be of intermediate age (Geisler et al. 1997, hereafter Paper I). This study increased considerably the known sample of 1 to 3 Gyr–old clusters with accurate age determinations, and it reinforced the conclusion that a major formation epoch was preceded by a quiescent period of many gigayears, or that cluster dissipation has been more effective than generally believed (e.g., Olszewski 1993).

The objective of the present paper is to compare the properties of outer LMC clusters with those of their surrounding fields by using the same observational technique and to infer the age-metallicity relation (and whether it depends on the spatial distribution throughout the LMC disk). In order to achieve this we employ Washington system CT_1 bands and construct CMDs using the data of Paper I. Ages are inferred from the difference δT_1 between the giant branch clump and the turnoff (see also Paper I), and from the occurrence of particular stellar evolutionary sequences in the CMDs. The giant and subgiant branches allow one to derive metallicities using a technique analogous to that of Da Costa & Armandroff (1990) for VI photometry. However, our combination of Washington system filters is 3 times more metallicity-sensitive than the VI system (Geisler & Sarajedini 1996, 1998), allowing us to obtain accurate metallicities for both the clusters and their fields. The cluster/field sample and the observations are described in § 2. The cluster and field CMDs are described in § 3. Ages and metallicities are derived in § 4. In § 5, we discuss the chemical enrichment of the outer disk, and in § 6 the presence of dual clumps in two fields is noted and the possibility of a depth effect in this portion of the LMC disk is discussed. Finally, the conclusions of this work are given in § 7.

2. SAMPLE AND OBSERVATIONS

The outer LMC disk is tilted at $i \approx 45°$ to the line of sight with the line of nodes at $\Theta \approx 7°$, as indicated by the distribution of outlying star clusters (Lyngå & Westerlund 1963; see also Westerlund 1990 for a review). The total observed sample of clusters was first reported in Paper I. In the present paper, we discuss in detail the 13 most distant outlying clusters from this sample and an additional inner cluster, SL 769, included for comparison purposes, and their respective 13 surrounding fields (IC 2134 and SL 451 are located in the same frame). The star cluster designations in different catalogs and respective B1950.0 equatorial coordinates are listed in Table 1. Galactic coordinates are also given in the table: since the distribution of the present clusters covers as much as 15° on the sky, variations of Galactic reddening are expected.

As a rule, the clusters are centered in the frames, with some exceptions that were shifted to avoid bright stars. In the case of IC 2134 and SL 451, the frame was centered approximately halfway between the two clusters, as illustrated in Figure 1, which also serves to illustrate typical clusters and field. The spatial distribution of the clusters is shown in Figure 2. With the exception of OHSC 37, which is located far east away from the disk body, the remaining clusters are consistent with an inclined disk as described above. We also show in Table 1 the approximate projected angular distance from the bar center (taken as the position of the cluster NGC 1928, $\alpha = 5^h21^m19^s$, $\delta = -69°31'30''$ [B1950.0]), which in turn is $\approx 0.°2$ south of the H I rotation curve center (see Westerlund 1990 for a review of centroids). Finally, the last column of Table 1 lists deprojected distances R, assuming that all clusters are part of the inclined disk.

The observations were carried out with the Cerro Tololo Inter-American Observatory (CTIO) 0.9 m telescope in 1996 December with the Tektronix 2K No. 3 CCD, as described in Paper I. The scale on the chip is $0''.40$ pixel^{-1}, yielding an area $13'.6 \times 13'.6$. SL 769 was observed with the CTIO 4 m in 1996 February with the Tektronix 2K No. 4 CCD, with similar pixel and areal coverage. The filters used for both runs were the Washington (Canterna 1976) C and Kron-Cousins R filters. The latter has significant throughput advantages over the standard Washington T_1 filter (Geisler 1996). In the present work, as in Paper I, we calibrate the observations in the CT_1 system. In particular, this filter combination allows us to derive accurate metallicities based on the standard giant branch technique outlined in Geisler & Sarajedini (1996, 1998). The data were reduced with the stand-alone version of DAOPHOT II (Stetson 1987), after trimming, bias subtraction, and flat-fielding.

TABLE 1

SAMPLE OF OUTLYING CLUSTERS AND SURROUNDING FIELDS

Star Cluster	α (B1950.0)	δ (B1950.0)	l (deg)	b (deg)	r (deg)	R (deg)
SL 8, LW 13	04 38 00	−69 07 37	280	−38.2	3.9	5.5
SL 126, ESO 85-SC21	04 56 53	−62 36 37	272.5	−36.9	7.5	8.0
SL 262, LW 146	05 08 52	−62 26 27	272.0	−36.0	7.2	7.4
SL 388, LW 186	05 19 44	−63 31 44	273.1	−34.2	6.0	6.0
IC 2134, SL 437, LW 198[a]	05 24 47	−75 29 26	287.1	−31.7	6.0	6.0
SL 451, LW 206[a]	05 25 57	−75 36 33	286	−31.6	6.1	6.1
SL 509, LW 221	05 29 29	−63 41 11	273.2	−33.1	5.9	6.0
SL 817	06 01 09	−70 04 07	280	−29.7	3.4	4.8
ESO 121-SC03	06 01 27	−60 31 17	269.5	−29.4	10.3	11.4
SL 842, LW 399	06 07 53	−62 58 40	272.3	−28.8	8.4	9.9
SL 862, LW 431	06 14 04	−70 40 45	281.1	−28.6	4.5	6.3
OHSC 33	06 16 33	−73 45 58	284	−28.5	5.7	6.9
OHSC 37	07 08 01	−69 54 10	280	−24.0	9.2	13.0
An Inner Disk Cluster						
SL 769[b]	05 53 54	−70 04 44	281	−30.3	2.8	4.0

NOTE.—Units of right ascension are hours, minutes, and seconds, and units of declination are degrees, arcminutes, and arcseconds.

[a] IC 2134 and SL 451 are located in the same frame.

[b] SL 769 is included for comparison purposes: Its location corresponds to the inner disk, i.e., in our definition when the mean field turnoff becomes as bright as the clump. This occurs at $R \sim 4°$ (see text).

More details on the observations, reductions, and calibration procedures are given in Paper I.

After deriving the photometry for all detected objects in each filter, a cut was made on the basis of the parameters returned by DAOPHOT. Only objects with $\chi < 2$, photometric error less than 2 σ above the mean error at a given magnitude, and $|\mathrm{SHARP}| < 0.5$ were kept in each filter (typically discarding about 10% of the objects), and then the remaining objects in the C and T_1 lists were matched with a tolerance of 1 pixel and raw photometry obtained. This raw photometry was then transformed to the standard Washington system, as outlined in Paper I. Final calibrated photometry for each cluster is given in Table 2.

We present the star cluster CMDs in Figure 3. The cluster radii were selected by eye-judging the variation of the stellar density in the cluster surroundings—and ranged from 50–200 pixels, with a typical value of 75 pixels (30″). These radii are intended to optimize the cluster CMD sequences to avoid field contamination as much as possible. The radius in pixels for the extraction of each cluster is indicated in the corresponding CMD in Figure 3.

We checked on the extent of field contamination of each cluster CMD by obtaining an equal-area field CMD composed of the addition of CMDs derived from four different fields, each of an area one-fourth that of the cluster and lying far away from the cluster. Note that such a comparison will overestimate field contamination, since the photometric limit within the cluster will be brighter than in the field, and more stars will be discarded from the cluster because of larger photometric errors due to increased crowding. Nevertheless, in only one outlying cluster was the number of stars obtained in the equal-area field significantly more than one-fourth of the stars in the cluster CMD. The typical ratio was only ~10%. Thus, we did not perform any statistical subtraction of the field contamination from the cluster CMDs.

We have also checked cluster extent on the basis of star counts and structural parameters and how it may be contributing to the surrounding fields in our frames. Three clusters in our sample have been studied by Kontizas, Hatzidimitriou, & Kontizas (1987), namely, SL 388 (LW 186), IC 2134 (LW 198), and SL 842 (LW 399), for which they could detect cluster stars as far as $r = 1.'4$, $1.'4$, and $1.'7$, respectively. Our selected radii for these clusters were $0.'5$, $0.'5$, and $0.'4$. Thus, our cluster radii are conservative and should minimize field contamination.

We have also obtained CMDs for each field excluding the pixels within a radius twice that used for the cluster, which minimizes contamination of the field by cluster stars. The tidal radii derived by Kontizas et al. (1987) for the three clusters ($r_t = 3'$, $6.'2$, and $3.'1$, respectively) are within the limits of the fields so defined. However, our criterion of field extraction is comparable to the detection limits of star counts, and the contribution of cluster stars to the field CMD (especially from clusters as relatively poorly populated as our sample) should not be significant. The tidal radius of ESO 121-SC03 is $2.'35$ according to Mateo, Hodge, & Schommer (1986). Note that the cluster CMD extraction (Fig. 3*i*) is for $r < 1.'33$, so that the field extraction corresponds to $r > 2.'67$, thus beyond the cluster tidal radius. The field CMDs are shown in Figure 4.

3. DESCRIPTION OF CMDS

The cluster CMDs (Fig. 3) are typical of intermediate-age clusters (IACs), with turnoffs ranging from magnitude levels slightly below the clump of He-burning stars to as much as 2 mag below. The only exception is ESO 121-SC03, which is considerably older. See Paper I for a discussion of the clump-to-turnoff magnitude difference and its relation to age.

3.1. *Fields*

The uniformly large size of the present frames is particularly suitable for the study of the brighter sequences of field stellar populations. The number of stars seen in the field CMDs (Fig. 4) is clearly correlated with the deprojected angular distances R from the bar center (Table 1). The radial dependence of several CMD features is also note-

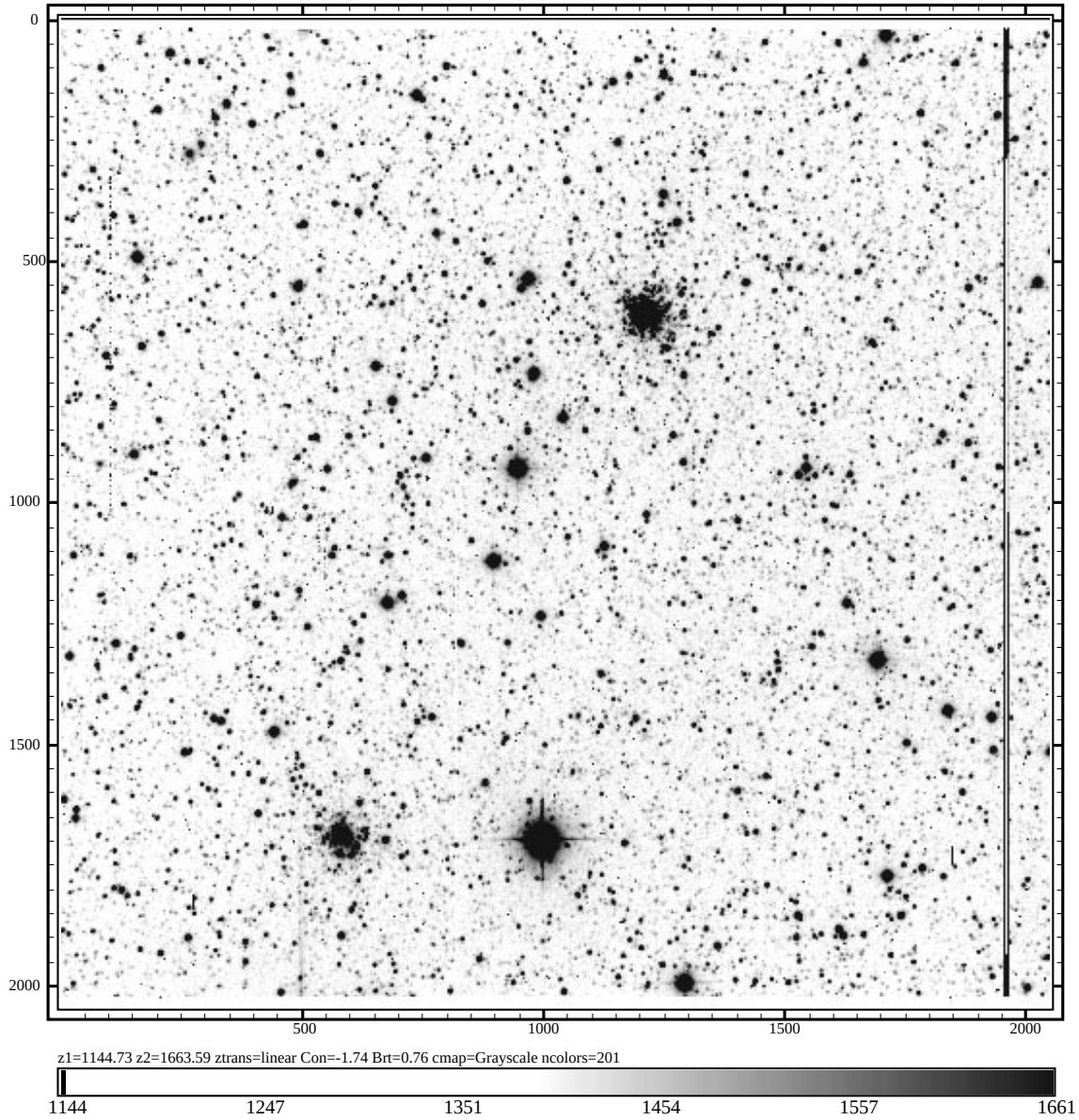

FIG. 1.—T_1 (R) frame of IC 2134 (*upper right cluster*) and SL 451. The field is 13.′6 on a side. North is up, and east is to the left.

worthy. The field of OHSC 37, at a distance $R = 13°$, has no evidence of a clump or horizontal branch or turnoff of any kind, so that no LMC field stellar populations are detected in this frame. The wide distribution of stars in the diagram essentially consists of foreground Galactic stars. Note that OHSC 37 is the most distant LMC cluster in the Olszewski et al. (1988) outer LMC cluster catalog. On the other hand, the field of ESO 121-SC03 presents clear clump and turnoff regions at the LMC distance. The $\delta T_1 \approx 2.9$ value is very similar to that of the cluster ESO 121-SC03 itself (Paper I), and thus both the cluster and LMC field have comparable ages ($\sim$9 Gyr) at this far-north locus with $R = 11.°4$. No evidence exists for any intermediate-age population in this field. One possibility is that the cluster and its surrounding field were a building block of the LMC, such as an accreted dwarf companion. Note that Galactic contamination is still important in this field.

Thus, we can detect the LMC field star population out to greater than 11° (the deprojected distance of ESO 121-SC03), or $\sim$11 kpc, but not to 13° ($\sim$13 kpc), despite the presence of clusters at this distance. This is in good agreement with previous estimates of the extent of the LMC and its cluster system (e.g., de Vaucouleurs 1955; Lyngå & Westerlund 1963; Olszewski et al. 1988).

The LMC becomes prominent relative to the Galactic field at distances $10° < R < 7°$ (e.g., the SL 126 and SL 842 fields), and the principal turnoff is still well below the clump ($\approx$2 mag). The oldest population is detectable by means of a concentration of stars near the instability strip locus faintward and blueward of the intermediate-age clump.

For less distant fields, the younger MS turnoff rapidly brightens, reaching the clump magnitude level for fields at $R \approx 5°$ (e.g., that of SL 8). The composite turnoff structure is obvious for such fields. Finally, the field of SL 769 at $R = 4°$ definitely has an important component with a blue MS brighter than that of the clump. We adopt this criterion as a definition of the inner LMC disk. In this inner disk field, a minor old component, as demonstrated by the horizontal-

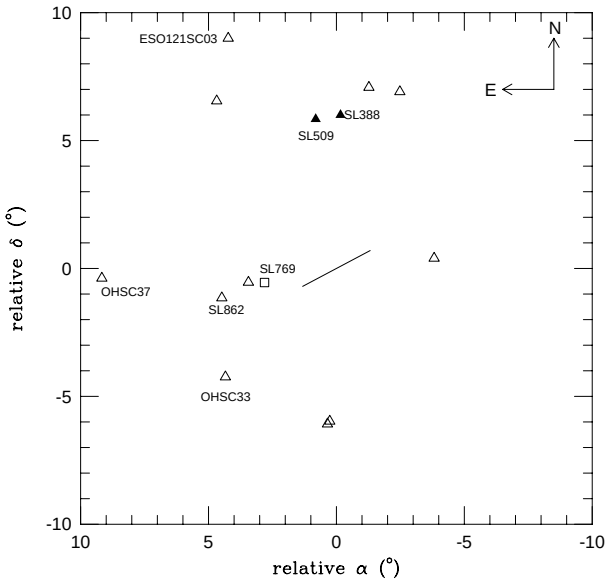

FIG. 2.—Spatial distribution of the sample. The LMC bar is schematically represented by a line, for comparison purposes. Clusters in the outer disk are shown as triangles. The fields of SL 388 and SL 509 (*filled triangles*) present an extra clump in the CMD, suggesting a depth structure (see § 6). The field of SL 769 (*square*) belongs to the inner disk.

branch (HB) stars faintward and blueward of the clump, is still present. The properties of our inner disk cluster sample and their fields will be the subject of a forthcoming paper.

4. DERIVATION OF AGES AND METALLICITIES

4.1. *Ages*

The utility of age determinations based on the magnitude difference between the clump/HB and the turnoff for IACs and old clusters is well known (see Phelps, Janes, & Montgomery 1994 for Galactic open clusters). In Paper I, we defined and calibrated such a method for δT_1 and applied it to our LMC cluster sample, including most of the present ones. In the present study, we have rigorously eliminated photometric outliers in individual CMDs. As a consequence, the CMDs were improved. We remeasured δT_1 values, and in some cases small differences appeared with respect to Paper I values. Such differences were almost always within the errors, averaging only 0.15 Gyr. Age determinations by two independent investigators yielded ages within 0.3 Gyr in the mean, with a standard deviation of 0.3 Gyr. We also ranked the clusters according to turnoff morphology and reddening-corrected magnitudes, taking into account the foreground $E(B-V)_G$ values (Table 4 below). The derived ages are given in Table 3. These values should be preferred over those given in Paper I.

Since the fields are in most cases obviously composite in age, we measure the δT_1 value of the youngest well-populated turnoff and use the age calibration from Paper I to derive the representative age given in Table 3. Although there are some fields with small numbers of younger stars, most of the stars in these fields are as old as or older than the given age. We cannot place any useful constraints on the proportion of turnoff stars in each field older than ~ 4 Gyr, as our photometry is not sufficient for the challenge. However, we do note that in the field with our deepest photometry (SL 769, obtained with the 4 m telescope), one can follow the subgiant branch down to a level that corresponds roughly to that shown by ESO 121-SC03, i.e., the faintest subgiants in the SL 769 field are consistent with an old (~ 9 Gyr) age. In some of the other fields, similarly faint subgiants can be seen. Comparing the ages for the clusters with the surrounding fields (as determined above), we conclude that they are similar, which suggests that, in general, the cluster has the same origin as the surrounding field population.

4.2. *Metallicities*

Da Costa & Armandroff (1990) showed the utility of the $V-I$ color of the red giant branch for measuring metallicities in old stellar populations. This method now sees very wide use and is the preferred technique, e.g., for *HST* Wide Field Planetary Camera 2 observations of the stellar populations in distant Galactic globular clusters and nearby galaxies.

Geisler (1994) and Geisler & Sarajedini (1996) introduced a similar technique using the $C - T_1$ color of the Washington system and demonstrated that it had much potential for deriving metal abundances in distant objects, with a metallicity sensitivity greatly exceeding that of $V-I$. Geisler & Sarajedini (1998) have now derived the calibration of the standard giant branches in the Washington system technique. They have used the mean loci of giant and subgiant branches of Galactic globular clusters and several old open clusters with known metallicities as fiducial clusters to derive the empirical relation between the $C - T_1$ color of the giant branch and metallicity, and they show that this technique has 3 times the sensitivity to metallicity that the corresponding $V-I$ technique has. The ability to derive accurate metallicities for our program clusters and fields using this new technique was one of our primary motivations for using the Washington system in the current study.

However, the fiducial clusters used by Geisler & Sarajedini (1998) are all either typical Galactic globular clusters, with ages of over 10 Gyr, or among the oldest open clusters (M67, with an age of ~ 4 Gyr, and NGC 6791, with an age of ~ 10 Gyr). In contrast, the only comparably aged cluster in the current sample is ESO 121-SC03—all of the rest are IACs ranging from ~ 1 to 2 Gyr. Given the noticeable effect of such a large age difference on broadband colors, the Geisler & Sarajedini calibration is not directly applicable to our sample. Instead, what we have chosen to do is to use the Geisler & Sarajedini fiducial loci to derive metallicities for a sample of LMC and Galactic open clusters of intermediate age and well-determined metallicity and then determine whether any offset is found between the known metallicity and the derived Washington value.

There are a total of five Galactic open clusters (Tombaugh 2, Melotte 71, NGC 2204, NGC 2506, and Melotte 66) and six LMC clusters (SL 262, SL 388, SL 842, NGC 2213, OHSC 33, and OHSC 37) that have both good Washington photometry available for a number of stars along the upper giant branch (either this paper, previous publications, or unpublished) and accurate metallicities (for the Galactic open clusters, these were taken from a variety of sources; for the LMC clusters, metallicities were taken from Olszewski et al. 1991). The ages of these clusters range from 1 to 4 Gyr.

In order to compare these clusters with the fiducial ones, a reddening and distance modulus were required to put the comparison clusters together with the standard ones in the $[M_{T_1}, (C - T_1)_0]$-plane. Again, for the Galactic open clus-

TABLE 2

WASHINGTON PHOTOMETRY

A. SL 8

ID	X	Y	T_1	$\sigma(T_1)$	$C - T_1$	$\sigma(C - T_1)$	CHI	SHARP
61.....	765.176	1056.106	16.069	0.006	3.216	0.015	1.035	0.148
767	839.763	884.935	18.544	0.013	1.600	0.021	0.922	0.000
145	796.596	889.515	16.799	0.004	2.690	0.010	0.905	0.000
10607.....	777.178	890.275	20.609	0.065	0.731	0.083	0.983	−0.370
527	776.272	900.708	18.160	0.010	2.031	0.022	1.008	−0.231
B. SL 126								
846	917.066	986.192	20.956	0.057	0.518	0.067	1.117	0.000
1831	862.959	987.215	21.775	0.083	0.668	0.108	0.910	0.056
1559	924.878	988.453	21.605	0.080	0.843	0.107	0.962	0.000
2052	905.857	989.342	22.114	0.103	0.960	0.153	0.857	−0.162
855	912.814	990.762	20.858	0.040	0.548	0.049	0.887	0.023
C. SL 162								
42.....	436.669	1690.165	16.270	0.006	2.953	0.059	1.110	0.027
885	449.608	1654.060	20.452	0.045	0.858	0.061	0.975	−0.062
1127	417.032	1654.185	20.873	0.061	0.619	0.076	0.935	−0.169
9273	433.216	1655.296	20.528	0.049	0.549	0.056	0.735	0.067
9282	401.921	1659.138	22.098	0.157	0.412	0.193	0.880	0.000
D. SL 388								
14278.....	843.816	960.332	22.110	0.144	0.558	0.177	0.875	−0.130
7502	877.592	961.537	21.320	0.077	0.400	0.089	0.920	0.000
3368	886.542	962.258	21.408	0.138	0.546	0.193	1.075	0.310
3526	904.402	963.581	21.411	0.100	0.725	0.131	1.060	−0.416
3490	884.844	964.969	21.431	0.141	0.913	0.219	1.000	−0.069
E. IC 2134								
1140	1211.969	547.030	19.223	0.019	1.704	0.070	1.035	0.002
1209	1230.870	553.348	19.804	0.030	0.369	0.054	0.885	−0.109
1794	1240.405	553.606	20.704	0.060	0.599	0.106	1.003	0.034
2186	1252.771	554.528	20.592	0.054	0.329	0.067	1.087	0.534
1144	1228.767	556.385	19.682	0.029	0.340	0.046	0.882	0.023
F. SL 451								
5254	581.516	1631.895	21.526	0.123	0.480	0.146	1.023	0.041
2197	595.337	1645.272	20.479	0.049	0.660	0.070	1.148	0.000
786	536.229	1649.193	18.697	0.010	1.660	0.021	0.883	0.000
1695	630.225	1649.831	20.010	0.034	0.328	0.039	0.928	0.185
4034	618.433	1650.073	20.823	0.059	0.737	0.078	0.931	−0.582
G. SL 509								
2268	891.183	915.843	14.972	0.004	3.666	0.031	0.770	−0.011
4182	877.170	919.187	20.651	0.074	0.390	0.089	1.005	0.000
4913	854.780	920.069	20.943	0.091	0.480	0.138	1.000	0.000
18721.....	887.715	920.105	20.501	0.099	0.050	0.104	0.625	0.075
18726.....	876.347	922.409	21.448	0.117	1.603	0.238	0.925	0.106
H. SL 817								
94.....	69.880	781.270	16.585	0.015	2.525	0.042	0.810	−0.060
12535.....	59.684	760.102	17.449	0.032	2.596	0.094	2.020	0.000
2767	65.824	722.092	20.566	0.051	0.979	0.069	1.005	−0.035
916	84.351	730.976	18.588	0.013	1.686	0.019	1.015	0.000
1433	57.680	733.382	18.748	0.012	1.815	0.023	0.975	−0.020
I. ESO 121-SC03								
11.....	1310.162	1208.792	15.816	0.006	3.030	0.020	1.839	0.187
16.....	1478.690	1208.884	16.025	0.005	2.966	0.023	1.934	0.314
701	1389.894	1029.254	20.679	0.037	1.233	0.059	1.035	0.000
1701	1355.332	1029.553	21.896	0.100	0.603	0.127	1.045	0.000
1631	1405.803	1035.728	21.918	0.095	0.646	0.127	0.997	−0.082

TABLE 2—*Continued*

ID	X	Y	T_1	$\sigma(T_1)$	$C-T_1$	$\sigma(C-T_1)$	CHI	SHARP
				J. SL 842				
139	58.866	1203.899	17.444	0.024	2.138	0.027	0.700	−0.032
1827	26.177	1150.098	20.988	0.089	0.468	0.098	0.850	0.000
1942	31.294	1154.331	20.920	0.076	0.420	0.095	1.025	0.000
1195	21.869	1155.128	20.507	0.063	1.146	0.102	1.190	0.157
1096	12.227	1156.701	20.281	0.066	1.119	0.080	1.140	−0.104
				K. SL 862				
9	487.976	634.438	15.210	0.010	3.220	0.029	1.434	0.000
53	508.772	605.333	16.431	0.013	2.719	0.026	0.766	0.000
82	483.662	641.473	16.732	0.011	2.454	0.021	1.127	0.000
15482	491.006	632.599	17.207	0.032	2.063	0.047	1.294	0.000
15259	467.353	575.511	21.535	0.090	0.378	0.105	0.859	0.106
				L. OHSC 33				
1306	1523.597	1558.571	20.929	0.056	0.345	0.066	0.836	−0.009
677	1518.475	1560.032	18.743	0.009	1.751	0.021	0.823	0.023
762	1503.499	1562.067	18.832	0.012	1.658	0.025	1.042	0.074
1372	1500.346	1566.467	20.923	0.065	0.407	0.077	0.791	0.001
2268	1513.518	1569.597	20.624	0.054	0.514	0.067	1.087	0.481
				M. OHSC 37				
56	808.438	969.282	16.653	0.018	2.980	0.021	1.398	0.052
1516	792.089	904.755	22.051	0.124	0.656	0.168	0.883	0.000
289	777.322	911.633	18.828	0.012	1.707	0.025	1.049	0.000
127	783.015	928.740	17.573	0.008	2.472	0.016	1.151	0.059
234	789.285	932.421	18.959	0.012	1.897	0.028	0.775	0.000
				N. SL 679				
9169	1020.291	930.753	20.410	0.044	1.238	0.053	0.995	0.000
25843	1064.183	930.779	21.676	0.120	0.640	0.124	0.766	0.125
8067	1053.189	930.803	20.400	0.027	0.635	0.052	1.113	0.090
17519	1049.711	931.219	21.194	0.057	0.641	0.079	1.479	0.266
13810	1016.177	932.326	20.846	0.090	0.639	0.092	1.240	0.000

NOTE.—Table 2 is presented in its entirety in the electronic edition of the Astronomical Journal. A portion is shown here for guidance regarding its form and content.

TABLE 3

AGES FOR CLUSTERS AND SURROUNDING FIELDS

Star Cluster	Age (Gyr)	
	Cluster	Field
SL 8, LW 13	1.8:	2.0[a]
SL 126, ESO 85-SC21	2.2	>2.5
SL 262, LW 146	2.1	2.0
SL 388, LW 186	2.2	2.0[a]
IC 2134, SL 437, LW 198	1.0	2.0
SL 451, LW 206	2.2	2.0
SL 509, LW 221	1.2	1.5[a]
SL 817	1.5:	2.0[a]
ESO 121-SC03	8.5	9.0
SL 842, LW 399	2.2:	2.5
SL 862, LW 431	1.8	2.0
OHSC 33	1.4	2.0
OHSC 37[b]	2.1:	...
An Inner Disk Cluster		
SL 769[c]	1.8	...

[a] A significant fraction of younger stars is present.

[b] The field population corresponds essentially to that of the Galaxy.

[c] The younger field turnoffs are younger than intermediate age (<1 Gyr) and outside of our age calibration.

ters we used the best current estimates available for these values based on an extensive literature search. For the LMC clusters, we assumed a true distance modulus $(m-M)_0 = 18.5$, taking into account results obtained from SN 1987A [$(m-M)_0 = 18.5$; Panagia et al. 1991] and the consequences of a recent revision of the Cepheid distance calibration on the LMC distance modulus [$(m-M)_0 = 18.50 \pm 0.15$; Madore & Freedman 1998]. The extent of the LMC outer disk is considerable, so we decided to use a foreground reddening $E(B-V)_G$ depending on the Galactic coordinates (Table 1) and the values from the maps by Burstein & Heiles (1982). The results are in Table 4. The reddening values for our entire LMC cluster sample vary from 0.00 to 0.10, except for OHSC 37, which is located at a lower Galactic latitude and consequently has a higher reddening. Since we are dealing with the outer LMC, the disk internal reddening is expected to be negligible. We note that an increase of the assumed reddening by $E(B-V) = 0.03$ decreases the derived metallicity (see below) by 0.12 dex.

We then derived metallicities for each of the 11 comparison clusters by interpolating by eye among the standard giant branches. Figure 5 shows the derived Washington metallicity versus the standard value taken from the liter-

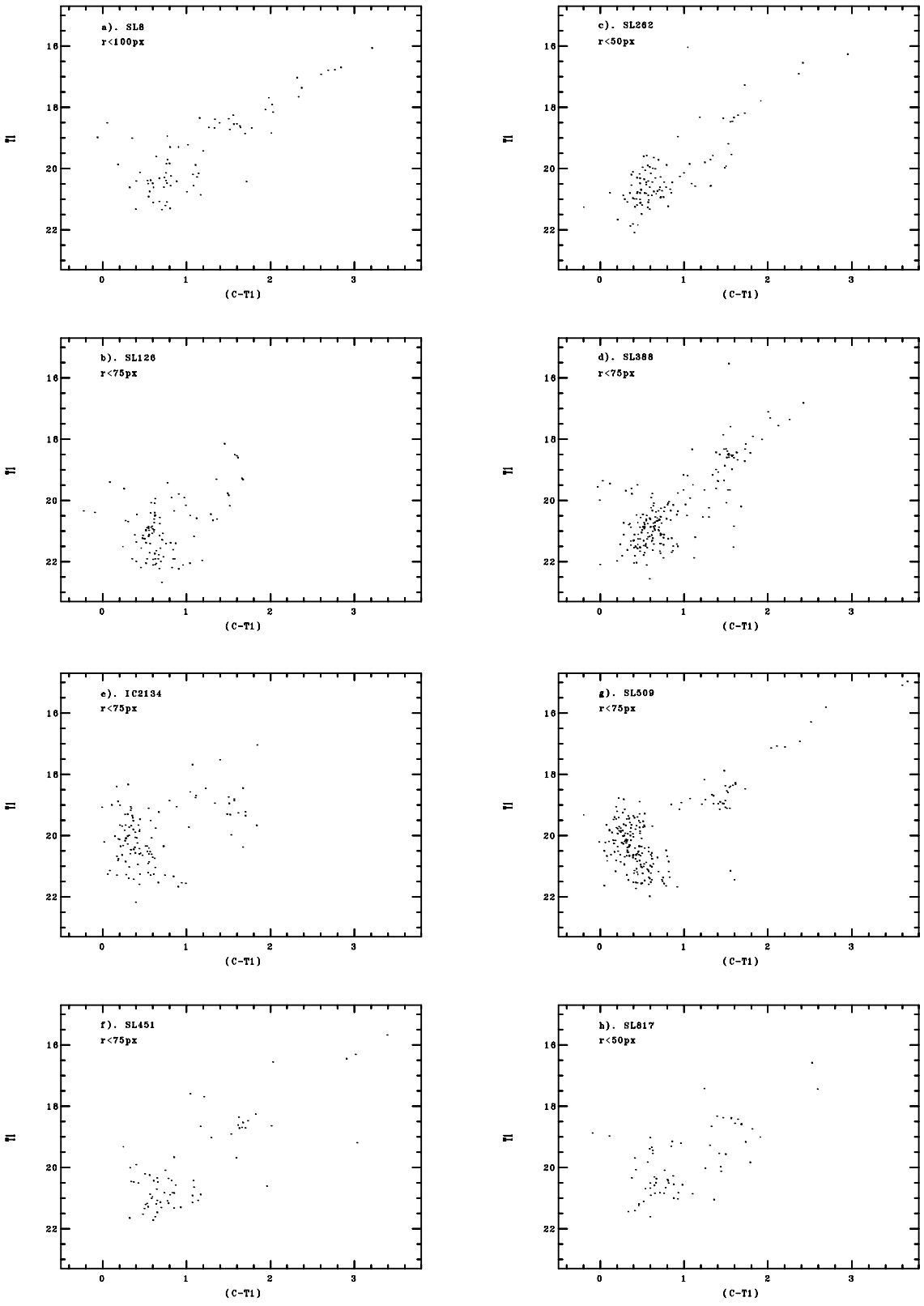

FIG. 3.—Washington T_1 vs. $C - T_1$ CMDs of the star clusters. The extraction radius in pixels is given in each panel. (*a*) SL 8; (*b*) SL 126; (*c*) SL 262; (*d*) SL 388; (*e*) IC 2134; (*f*) SL 451; (*g*) SL 509; (*h*) SL 817; (*i*) ESO 121-SC03; (*j*) SL 842; (*k*) SL 862; (*l*) OHSC 33; (*m*) OHSC 37; (*n*) SL 769.

ature. A clear trend is found, indicating that the derived Washington metallicities for IACs using this technique require an approximately constant zero-point correction. An unweighted mean yields a difference of 0.41 $\pm$ 0.21 dex. We then determined the metallicity of all of our program LMC clusters and fields in the same manner and applied an offset of 0.4 dex to the derived value, i.e., we increased our estimate derived from a direct comparison with the stan-

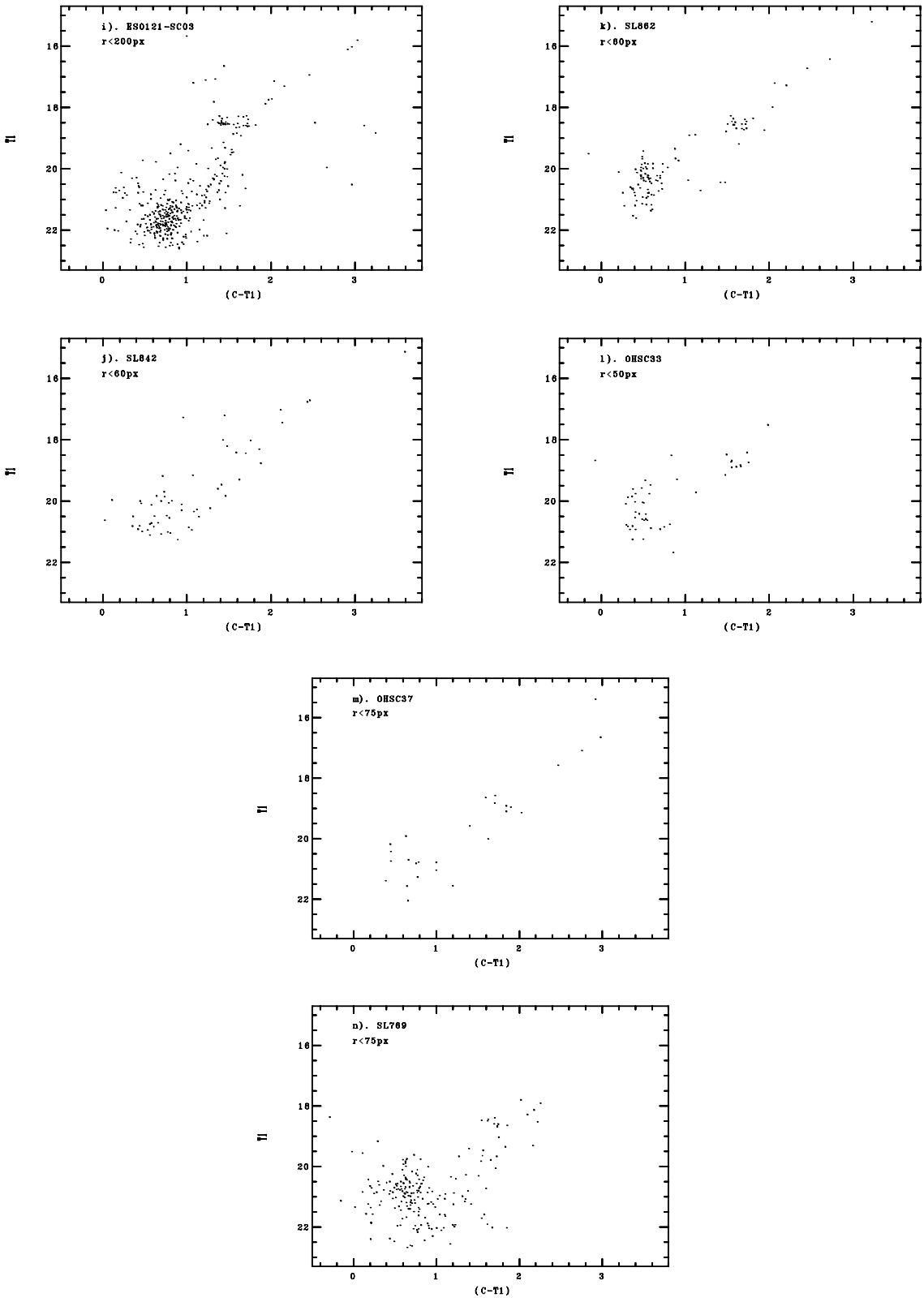

FIG. 3.—*Continued*

dard clusters by 0.4 dex. Figure 6 shows a typical IAC, and Figure 7 a typical IAC field. The final corrected values are given in Table 4. In a few cases, the metallicities were difficult or virtually impossible to determine, because of the lack of bright giants—these cases are marked with colons or dashes in the table, and any derived metallicities are more uncertain. Note that the fields generally showed a significant range in metallicity, amounting to ~ 0.5 dex (although some of this scatter can be explained by Galactic field star contamination or LMC asymptotic giant branch stars), and

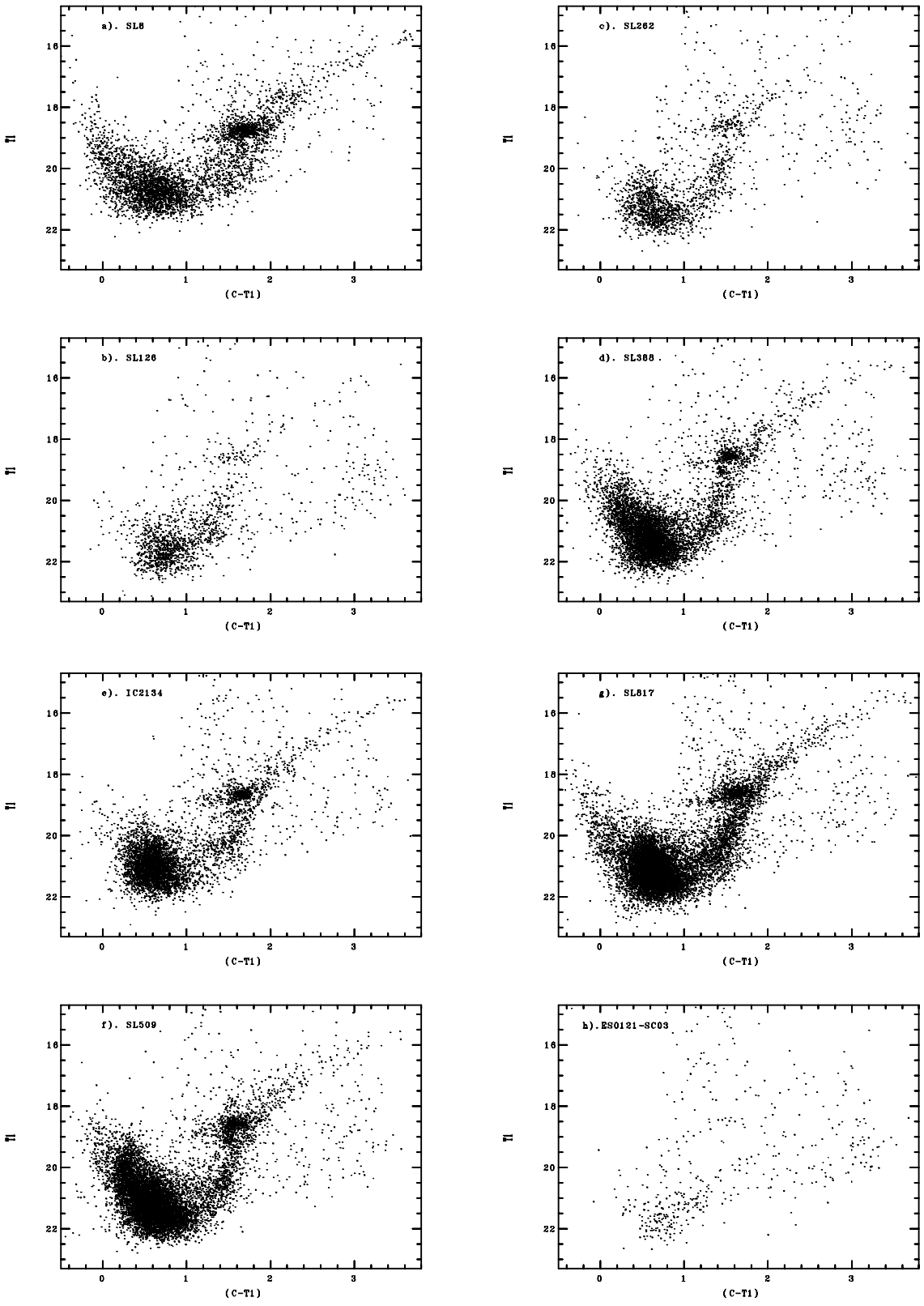

FIG. 4.—Washington T_1 vs. $C - T_1$ CMDs of the surrounding fields, excluding areas of radius 2 times that of the cluster. (*a*) SL 8; (*b*) SL 126; (*c*) SL 262; (*d*) SL 388; (*e*) IC 2134; (*f*) SL 509; (*g*) SL 817; (*h*) ESO 121-SC03; (*i*) SL 842; (*j*) SL 862; (*k*) OHSC 33; (*l*) OHSC 37; (*m*) SL 769.

that the values quoted are crude means. The offset is required for any intermediate-age objects, which is the case for all but one of our LMC clusters and most of the field stars. However, note that our value for ESO 121-SC03, as derived from Figure 8, has not been corrected, since this is an old cluster. Our derived metallicity is only 0.12 dex lower than that of Olszewski et al. for this cluster, showing good agreement. In the case of any field stars that are significantly

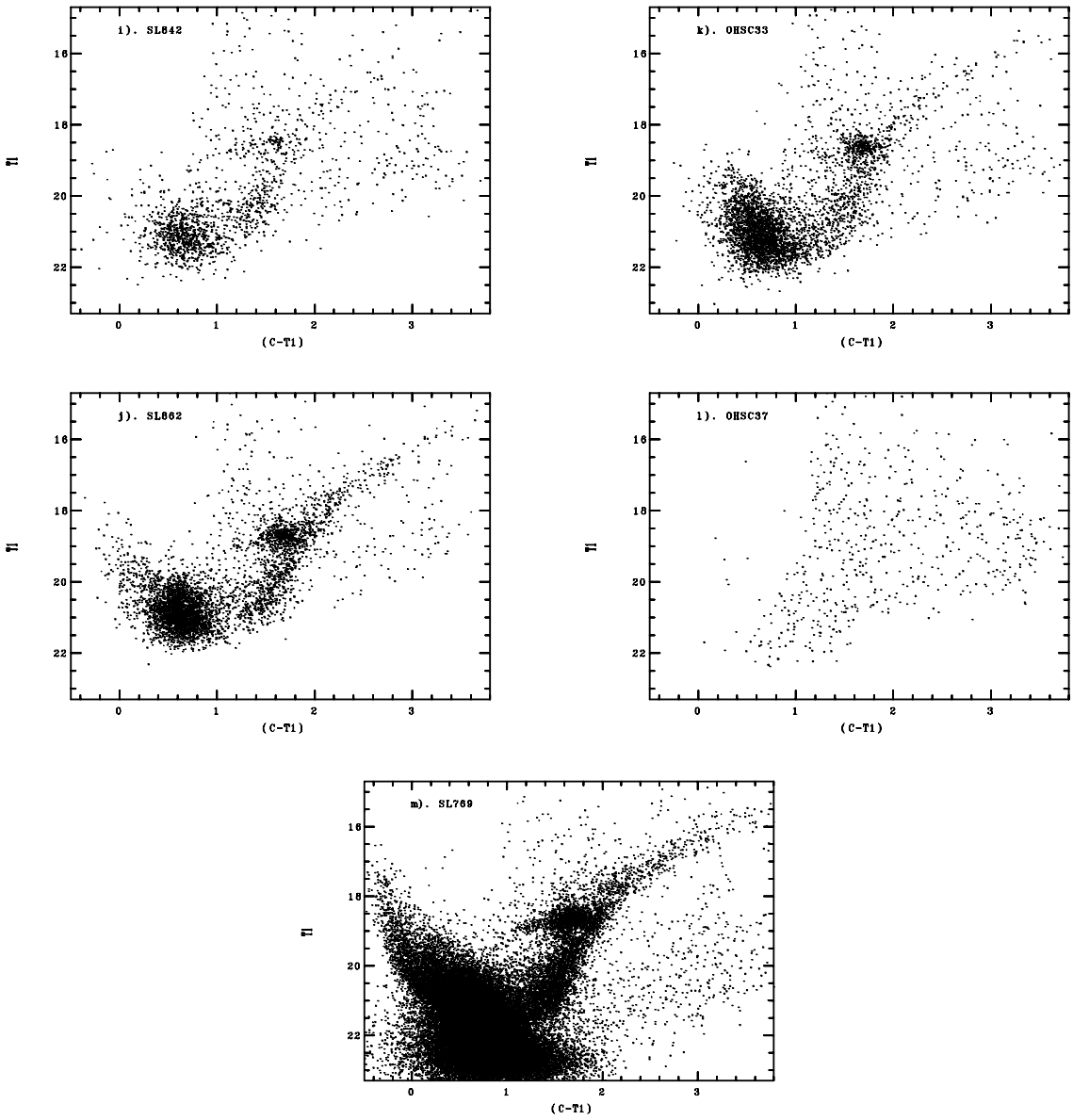

FIG. 4.—*Continued*

older than ~4 Gyr, our corrected metallicity will represent an overestimate. However, such stars appear to be a very small minority in our fields.

In order to obtain an estimate of the errors involved in the metallicity derived from our interpolation procedure, two of us made independent measurements. We got the following differences: for metallicities of clusters and fields, $\langle [Fe/H]_{E.B.} - [Fe/H]_{D.G.} \rangle = -0.05$, with $\sigma = 0.07$; for the metallicity difference between cluster and respective field, $\langle \Delta[Fe/H]_{E.B.} - \Delta[Fe/H]_{D.G.} \rangle = -0.07$, with $\sigma = 0.13$ for 12 field/cluster CMDs. Therefore, we estimate that our internal metallicity errors are of order 0.1 dex, and that the total metallicity uncertainties are ~0.2 dex.

Table 4 also lists the Olszewski et al. metallicity values for clusters in common. For these seven clusters, we derive a mean difference of 0.09 dex (our values are more metal-rich), with $\sigma = 0.34$ dex. Given that their errors are similar to ours, this is exactly the value expected if no other sources of error are present. Of course, we have used five of these clusters to derive the offset, but these represented less than half the total number of clusters used.

5. CHEMICAL ENRICHMENT

Olszewski et al. (1991) studied the chemical enrichment of the LMC, based on ages from CMDs and metallicities derived from Ca II triplet spectroscopy of some individual giants. They obtained $\langle [Fe/H] \rangle = -0.42$ for 17 clusters with ages in the same range as for our sample (1–3 Gyr). In Paper I, we increased the sample of well-studied IACs by combining ages from new CMDs with metallicities from Olszewski et al. (1991). We found evidence of a larger dispersion of metallicities at intermediate ages, in the sense that some outer clusters were more metal-poor than the average. In the present study, we revisit this issue for our outer disk sample and their fields, using the ages and metallicities derived here. Our method relies on a larger number of stars per cluster (Olszewski et al. generally observed only about two stars per cluster, while we generally have five or

TABLE 4

REDDENINGS AND METALLICITIES FOR CLUSTERS AND SURROUNDING FIELDS

STAR CLUSTER	$E(B-V)_G$	CLUSTER [Fe/H]		FIELD [Fe/H]
		This Paper	Olszewski et al.	
SL 8, LW 13	0.04	−0.5	...	−0.35
SL 126, ESO 85-SC21	0.01	−0.45:	−1.18:	−0.45
SL 262, LW 146	0.00	−0.55	−0.34	−0.5:
SL 388, LW 186	0.03	−0.65	−0.76	−0.6
IC 2134, SL 437, LW 198	0.10	...	...	−0.7
SL 451, LW 206	0.10	−0.7:	...	...
SL 509, LW 221	0.03	−0.85	...	−0.5
SL 817	0.07	−0.5:	...	−0.7
ESO 121-SC03	0.03	−1.05	−0.93	...
SL 842, LW 399	0.03	−0.6	−0.36	−0.55:
SL 862, LW 431	0.09	−0.85	...	−0.6
OHSC 33	0.09	−1.0:	−1.07:	−0.65
OHSC 37	0.15	−0.65	−0.91	...
An Inner Disk Cluster				
SL 769	0.08	−0.5	...	−0.55

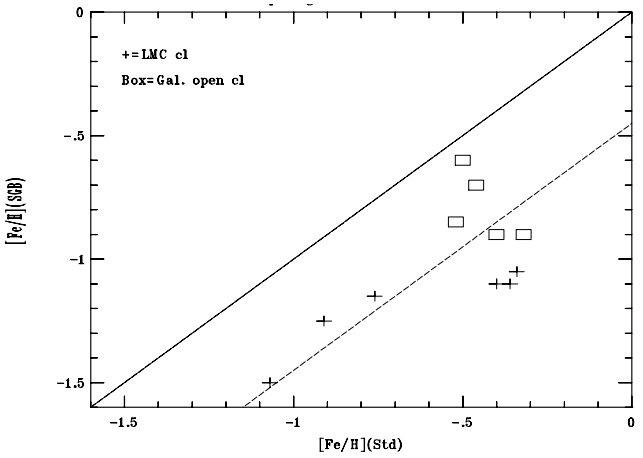

FIG. 5.—Metallicity derived from the color of the giant branch in the Washington system—compared with standard giant branches vs. standard metallicity. Plus signs are LMC clusters, squares are Galactic open clusters. The solid line shows perfect correlation; the dashed line indicates the mean relation we find: $[Fe/H]_{STD} = [Fe/H]_{SGB} + 0.4$.

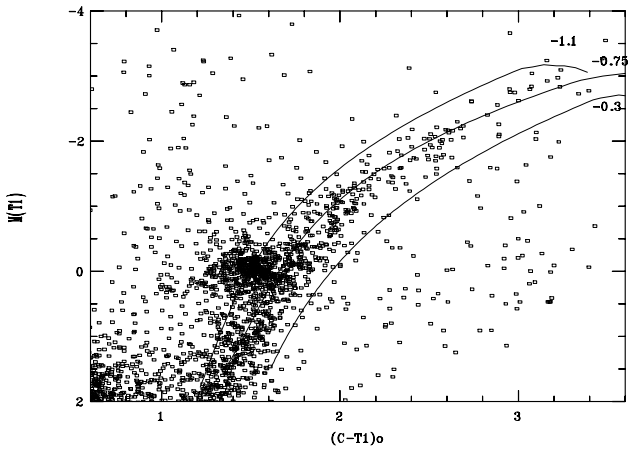

FIG. 7.—Same as Fig. 6, but for the field of SL 862, with the addition of the standard giant branch for 47 Tuc (offset [Fe/H] = −0.3).

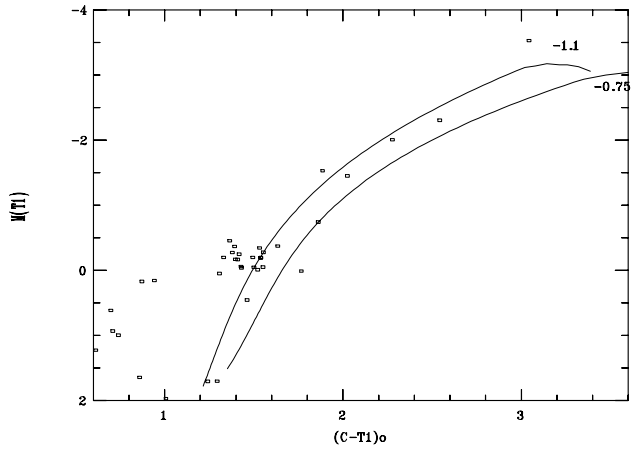

FIG. 6.—Metallicity derivation for the IAC SL 862. The cluster has been placed in the absolute T_1-magnitude vs. dereddened $C - T_1$ color plane, assuming a true distance modulus of 18.5 and a reddening of $E(B-V) = 0.09$. The standard giant branches are those of NGC 6752 (offset [Fe/H] = −1.1) and NGC 1851 (offset [Fe/H] = −0.75).

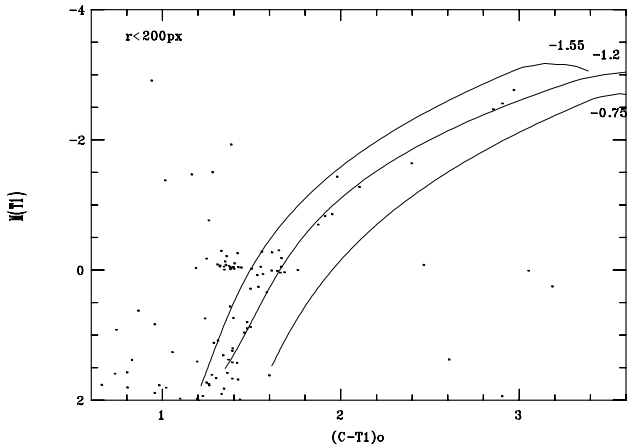

FIG. 8.—Same as Fig. 7, but for the old cluster ESO 121-SC03. Here the standard, not offset, metallicities are shown.

more to determine the giant branch locus); the relative metallicity errors are similar.

The results are shown in Figure 9, where we plot clusters and fields, as well as some LMC globular clusters for comparison purposes (Paper I and references therein), and the mean curve for IACs derived by Olszewski et al. The resulting enrichment scenario we find for the outer disk is that of a preenriched gas with metallicity about 1/10 solar (the metallicity level of ESO 121-SC03 in the quiescent epoch). Most parts of the outer disk were enriched by ≈ 0.3 dex before or during the burst that formed the IACs, but some regions apparently remained at the preenrichment level, forming some clusters with [Fe/H] ≈ -1.0 even at later stages of the burst. Alternatively, such clusters might have been formed elsewhere and are presently superposed or embedded in slightly more metal-rich outer disk fields (see discussion in Paper I). Indeed, Figure 9 reveals a considerable range of metallicities for the IACs ($-0.45 >$ [Fe/H] > -1.0), whereas the fields cover only half this range ($-0.35 >$ [Fe/H] > -0.7). The clusters responsible for the metallicity dispersion are SL 509, SL 862, and OHSC 33, which have ≈ 0.3 dex lower metallicities than the respective fields. Note that SL 509 is not only metal-poor but also very young, and that it exhibits the dual clump discussed in § 6. OHSC 33 is also intriguing as another young, metal-poor cluster. The metallicity we derive for it is virtually identical to that found by Olszewski et al. However, for most of the sample, clusters and fields have comparable properties. The mean metallicity of the 11 IACs in the outer disk is $\langle$[Fe/H]$\rangle = -0.66 \pm 0.17$, while for the fields it is $\langle$[Fe/H]$\rangle = -0.56 \pm 0.11$. A direct comparison shows that the clusters are essentially all slightly more metal-poor than their respective fields, with a mean difference of 0.12 dex. Thus, the clusters and their fields have very similar metallicities.

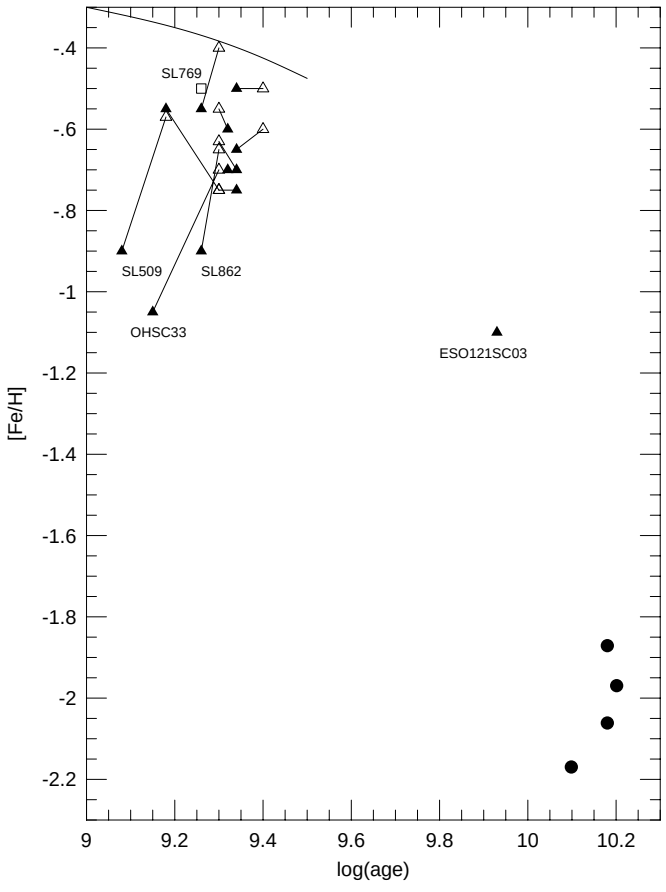

FIG. 9.—Chemical evolution of the LMC outer disk: open triangles refer to fields, filled triangles to clusters. Lines link cluster and the respective surrounding field. For comparison purposes, we show some LMC globular clusters (*circles*) and an LMC inner disk cluster (*square*). The age for the field corresponding to SL 126, located at (9.4, −0.5), is a lower limit (Table 3). The curve shows the mean age-metallicity relation derived by Olszewski et al. (1991) for IACs. Metallicities for our sample should be increased by +0.05 dex.

The IACs in the present sample are on average 0.24 dex more metal-poor than clusters of similar age in the Olszewski et al. (1991) sample. We have already shown that clusters in common yield similar metallicities. Probably, our lower average metallicity is real and reflects a gradient between the outer and inner regions of the LMC (see also Paper I). Figure 10 plots metallicity versus deprojected radius R for both the clusters and fields in our sample. No strong trend emerges, but as noted by Olszewski et al., there is a tendency for the most distant clusters to be more metal-poor. Note that Olszewski et al. did uncover ~ 10 IACs with metallicities less than -0.75, but their ages were mostly unavailable, so they were not included in their age-metallicity relation.

Traditionally, the young (< 1 Gyr) LMC population has been found to have a metallicity only slightly (~ 0.2 dex) less than solar (e.g., Harris 1983; Russell & Bessell 1989). IACs are generally regarded as having only slightly lower metallicities ([Fe/H] ~ -0.4), mostly based on the work of Olszewski et al. However, a number of studies have suggested that lower metallicities for such objects might be more appropriate. In an early study including a large sample of IACs using narrowband integrated photometry, Bica, Dottori, & Pastoriza (1986) derived metallicities similar to the present ones. Although ages for LMC IACs in that study were mostly based on LMC calibrators available at that time and require revision, the metallicities were derived from reference Galactic open and globular clusters with accurate abundances. Richtler, Spite, & Spite (1989) and Richtler (1993) derived values of -0.7 to -0.9 for several young LMC clusters using Strömgren photometry and high-resolution spectroscopy. Vallenari et al. (1991) found a metallicity of -0.6 for the IAC NGC 2164. As for the LMC field, there are also several recent indications that we may

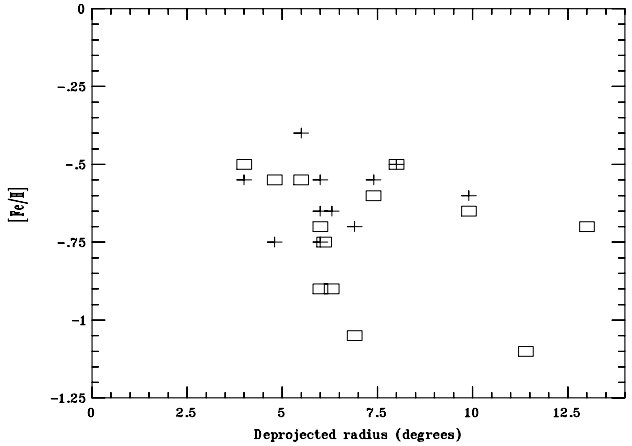

FIG. 10.—Metallicity vs. deprojected radius for LMC outer clusters (*squares*) and fields (*plus signs*). The point at the bottom right is ESO 121-SC03. Metallicities should be increased by +0.05 dex.

need to revise metallicity estimates downward. Geha et al. (1998) found that very low metallicities ($\lesssim -1$) are required to fit the giant branch colors in their *HST* fields, and Alves et al. (1998) analyzed MACHO project photometry for $\sim 10^7$ stars in the bar and found that a two-component model best fits the observations, with the intermediate-age component having a metallicity of about -0.7.

Thus, we conclude that intermediate-age LMC clusters and fields, especially in the outer disk, may be more metal-poor than previously generally regarded. More spectroscopic and photometric studies with a large number of giants per cluster for a larger sample of IACs would help clarify this question.

6. DUAL CLUMPS

The fields of SL 388 and SL 509 (Fig. 4), located together in the northern part of the LMC (Fig. 2), present a unique feature: a populated secondary clump ≈ 0.45 mag fainter than the prominent main clump seen in all other fields. This fainter clump in the CMD is also slightly bluer, which suggests a lower metallicity, older age, or both. The lower clump stars are found uniformly across both fields. This feature might be interpreted as a depth structure consisting of a layer of stars located approximately 10 kpc behind the LMC, at a distance comparable to that of the SMC. The fact that the fields of SL 509 and SL 388 are separated by only $\approx 1°$ on the sky sets a lower limit to the size of that possible structure of about 1 kpc. An alternative explanation might be the presence of a dwarf companion to the LMC. In the SMC, the occurrence of depth effects is well documented both in the field stellar component (Hatzidimitriou & Hawkins 1989) and in velocity space for the H I distribution (Mathewson & Ford 1984). A stellar bridge exists between the Clouds, having arisen from their past interaction (Irwin, Demers, & Kunkel 1990), and two concentrations in the bridge and one in the extreme of the SMC wing may evolve into dwarf galaxies (Bica & Schmitt 1995). All this evidence suggests that depth effects or dwarf galaxies might also occur elsewhere in the Magellanic System, as debris from interactions. Note, however, that these two clusters lie at the very outer limit of the H I distribution of Mathewson & Ford (1984).

Arguments against this interpretation are that, if it is a superposition of two similar populations at different distances, one would expect at least greater scatter in the principal CMD sequences, yet this is not the case. More importantly, SL 509 itself shows the same dual clump, with the fainter clump even more pronounced with respect to the brighter clump than seen in the field CMD, and an equal-area field reinforces this. Also, there is a hint of a dual clump in the very populous SL 769 field, located many degrees away. Finally, a similar feature is perhaps present in the Galactic open cluster NGC 2243 (Bonifazi et al. 1990). More studies are needed to investigate this intriguing feature.

7. CONCLUSIONS

By using Washington system color-magnitude diagrams of a large sample of IACs and their surrounding fields in the LMC outer disk, we are able to derive ages and metallicities. The cluster stellar population is a major component of the field where it is embedded, thus sharing its mean age and metallicity properties, except in three cases where the clusters are ≈ 0.3 dex more metal-poor than the field, suggesting that the chemical enrichment was not globally homogeneous in the LMC. Our data are consistent with a scenario in which local star formation events generated both the clusters and a significant part of their surrounding stellar fields. Thus, during the last 1–3 Gyr the dynamical evolution of the disk has not significantly taken them apart, which provides information on the diffusion timescale and mixing of stellar generations in the disk. The old population ($t \geq 10$ Gyr) is detected in most fields as a small concentration of stars on the horizontal branch blueward and faintward of the prominent clump.

The unique cluster ESO 121-SC03 at ≈ 9 Gyr has a surrounding field that shares the same stellar population. No other field so far studied is dominated by such an old population. One possibility would be that a field and cluster population coupling might last that long. Alternatively, we might be dealing with a building block recently accreted by the LMC in the form of a dwarf galaxy.

One IAC cluster (OHSC 37) is so far from the LMC body that no surrounding LMC field is detected. The present observations suggest that the LMC stellar disk extends out to between ~ 11 and 13 kpc in deprojected radius. In the northern part of the LMC outer disk, the fields of SL 388 and SL 509 present evidence of a depth effect with a secondary component located behind the LMC disk at a distance comparable to that of the SMC. A background layer of stars was possibly detected, and its size is at least ≈ 1 kpc, comparable to that of a dwarf galaxy. The peculiar location of the cluster OHSC 37 and the depth effect in the SL 388 and SL 509 fields might be explained as debris from previous interactions of the LMC with the Galaxy and/or the SMC.

The average metallicity derived for the present outer disk IACs is $\langle [Fe/H] \rangle = -0.66 \pm 0.17$, and for their surrounding fields is $\langle [Fe/H] \rangle = -0.56 \pm 0.11$. A few clusters stand out in the age-metallicity relation, in the sense that they are intermediate-age clusters at [Fe/H] ≈ -1. The outer LMC disk (clusters and fields), at least of this age range (1–3 Gyr), seem to be more metal-poor than previously generally regarded.

The authors would like to thank Cristina Torres for providing data critical to the metallicity calibration in advance of publication. E. Geisler, as always, was an inspiration. Support for this work was provided in part by NASA through grant GO-06810.01-95A (to D. G.) from the Space Telescope Science Institute, which is operated by the Association of Universities for Research in Astronomy, Inc., under NASA contract NAS 5-26555. This work was partially supported by the Brazilian institutions CNPq and FINEP, the Argentine institutions CONICET and CONICOR, and the Vitae and Antorcha Foundations.

REFERENCES

Alves, D., et al. 1998, BAAS, in press
Bertelli, G., Mateo, M., Chiosi, C., & Bressan, A. 1992, ApJ, 388, 400
Bica, E., Clariá, J. J., & Dottori, H. 1992, AJ, 103, 1859
Bica, E., Clariá, J. J., Dottori, H., Santos, J. F., Jr., & Piatti, A. E. 1996, ApJS, 102, 57
Bica, E., Dottori, H., & Pastoriza, M. 1986, A&A, 156, 261
Bica, E., & Schmitt, H. R. 1995, ApJS, 101, 41
Bonifazi, A., Fusi Pecci, F., Romeo, G., & Tosi, M. 1990, MNRAS, 245, 15
Burstein, D., & Heiles, C. 1982, AJ, 87, 1165
Butcher, H. 1977, ApJ, 216, 327

Canterna, R. 1976, AJ, 81, 228
Da Costa, G. S. 1991, in IAU Symp. 148, The Magellanic Clouds, ed. R. Haynes & D. Milne (Dordrecht: Kluwer), 145
Da Costa, G. S., & Armandroff, T. E. 1990, AJ, 100, 162
de Vaucouleurs, G. 1955, ApJ, 60, 126
Dottori, H., Bica, E., Clariá, J. J., & Puerari, I. 1996, ApJ, 742, 100
Elson, R. A. W., Gilmore, G. F., & Santiago, B. X. 1997, MNRAS, 289, 157
Gallagher, J. S., et al. 1996, ApJ, 466, 732
Geha, M. C., et al. 1998, AJ, 115, 1045
Geisler, D. 1994, in Third CTIO/ESO Workshop on the Local Group, ed. A. Layden, R. C. Smith, & J. Storm (Garching: ESO), 141
———. 1996, AJ, 111, 480
Geisler, D., Bica, E., Dottori, H., Clariá, J. J., Piatti, A. E., & Santos, J. F. C., Jr. 1997, AJ, 114, 1920 (Paper I)
Geisler, D., & Sarajedini, A. 1996, in ASP Conf. Ser. 92, Formation of the Galactic Halo—Inside and Out, ed. H. L. Morrison & A. Sarajedini (San Francisco: ASP), 524
———. 1998, AJ, submitted
Girardi, L., & Bica, E. 1993, A&A, 274, 279
Girardi, L., Chiosi, C., Bertelli, G., & Bressan, A. 1995, A&A, 298, 87
Hardy, E., Buonanno, R., Corsi, C. E., Janes, K. A., & Schommer, R. A. 1984, ApJ, 278, 592
Harris, H. C. 1983, AJ, 88, 507
Hatzidimitriou, D., & Hawkins, M. R. S. 1989, MNRAS, 241, 667
Hodge, P. W. 1989, ARA&A, 27, 139
Holtzman, J. A., et al. 1997, AJ, 113, 656
Irwin, M. J., Demers, S., & Kunkel, W. E. 1990, AJ, 99, 191
Kontizas, M., Hatzidimitriou, D., & Kontizas, E. 1987, A&AS 68, 493
Lyngå, G., & Westerlund, B. E. 1963, MNRAS, 127, 31
Madore, B., & Freedman, W. 1998, ApJ, 492, 110
Mateo, M., Hodge, P., & Schommer, R. A. 1986, ApJ, 311, 113
Mathewson, D. S., & Ford, V. L. 1984, in IAU Symp. 108, Structure and Evolution of the Magellanic Clouds, ed. S. van den Bergh & K. S. de Boer (Dordrecht: Reidel), 125
Olszewski, E. W. 1993, in ASP Conf. Ser. 48, The Globular Cluster–Galaxy Connection, ed. G. H. Smith & J. P. Brodie (San Francisco: ASP), 351
Olszewski, E. W., Harris, H. C., Schommer, R. A., & Canterna, R. W. 1988, AJ, 95, 84
Olszewski, E. W., Schommer, R. A., Suntzeff, N. B., & Harris, H. C. 1991, AJ, 101, 515
Olszewski, E. W., Suntzeff, N. B., & Mateo, M. 1996, ARA&A, 34, 511
Panagia, N., Gilmozzi, R., Macchetto, F., Adorf, H.-M., & Kirshner, R. P. 1991, ApJ, 380, L23
Phelps, R. L., Janes, K. A., & Montgomery, K. A. 1994, AJ 107, 1079
Richtler, T. 1993, in ASP Conf. Ser. 48, The Globular Cluster–Galaxy Connection, ed. G. H. Smith & J. P. Brodie (San Francisco: ASP), 375
Richtler, T., Spite, M., & Spite, F. 1989, A&A, 225, 351
Russell, S. C., & Bessell, M. S. 1989, ApJS, 70, 865
Stetson, P. B. 1987, PASP, 99, 191
Suntzeff, N. B., Schommer, R. A., Olszewski, E. W., & Walker, A. W. 1992, AJ, 104, 1743
Vallenari, A., Chiosi, C., Bertelli, G., Aparicio, A., & Ortolani, S. 1996, A&A, 309, 367
Vallenari, A., Chiosi, C., Bertelli, G., Meylan, G., & Ortolani, S. 1991, A&AS, 87, 517
Westerlund, B. E. 1990, A&A Rev., 2, 29
Westerlund, B. E., Linde, P., & Lyngå, G. 1995, A&A, 298, 39

Note added in proof.—Girardi et al. (astro-ph/9805127) have used population synthesis and theoretical models to study the details of red giant clump stars and found evidence for a second clump blueward and faintward of the prominent red clump. Such a feature matches qualitatively the dual clumps seen here in several of our fields. However, the lack of such structure in other, more populous, fields is then unexplained.